Human Asunder promotes dynein recruitment and centrosomal tethering to the nucleus at mitotic entry

Jeanne N. Jodoin[a], Mohammad Shboul[b], Poojitha Sitaram[a], Hala Zein-Sabatto[a], Bruno Reversade[b,c], Ethan Lee[a], and Laura A. Lee[a]

[a]Department of Cell and Developmental Biology, Vanderbilt University Medical Center, Nashville, TN 37232-8240; [b]Institute of Medical Biology, A*STAR, Singapore, Singapore 138648; [c]Department of Pediatrics, National University of Singapore, Singapore 119228

ABSTRACT **Recruitment of dynein motors to the nuclear surface is an essential step for nucleus–centrosome coupling in prophase. In cultured human cells, this dynein pool is anchored to nuclear pore complexes through RanBP2–Bicaudal D2 (BICD2) and Nup133– centromere protein F (CENP-F) networks. We previously reported that the *asunder* (*asun*) gene is required in *Drosophila* spermatocytes for perinuclear dynein localization and nucleus–centrosome coupling at G2/M of male meiosis. We show here that male germline expression of mammalian Asunder (ASUN) protein rescues *asun* flies, demonstrating evolutionary conservation of function. In cultured human cells, we find that ASUN down-regulation causes reduction of perinuclear dynein in prophase of mitosis. Additional defects after loss of ASUN include nucleus–centrosome uncoupling, abnormal spindles, and multinucleation. Coimmunoprecipitation and overlapping localization patterns of ASUN and lissencephaly 1 (LIS1), a dynein adaptor, suggest that ASUN interacts with dynein in the cytoplasm via LIS1. Our data indicate that ASUN controls dynein localization via a mechanism distinct from that of either BICD2 or CENP-F. We present a model in which ASUN promotes perinuclear enrichment of dynein at G2/M that facilitates BICD2- and CENP-F-mediated anchoring of dynein to nuclear pore complexes.**

Monitoring Editor
Yixian Zheng
Carnegie Institution

Received: Jul 27, 2012
Revised: Oct 9, 2012
Accepted: Oct 16, 2012

INTRODUCTION

Cytoplasmic dynein plays critical roles in many cellular processes by carrying out minus end–directed transport along microtubules (Holzbaur and Vallee, 1994). Dynein is a multimeric complex composed of heavy, intermediate, light intermediate, and light chains. Each heavy chain contains six ATPase domains that power the motor. Noncatalytic subunits regulate dynein by linking the complex to its cargo and adaptor proteins. Dynein complexes approach 2 MDa in size, making dynein the largest of all known motor complexes. The composition of dynein complexes and the cellular events requiring these complexes have been defined, although a comprehensive understanding of the mechanisms by which these complexes are regulated within cells is lacking.

Dynein complexes are subject to several modes of regulation, including phosphorylation, subunit composition, subcellular localization, and binding of accessory proteins. Dynactin, another large multimeric complex, was identified through in vitro studies as an activator of dynein; subsequent work suggested that dynein requires dynactin to perform its cellular functions (Schroer, 2004). A dynein adaptor protein, lissencephaly 1 (LIS1), binds directly to dynein heavy chains and is essential for multiple dynein functions, including coupling of centrosomes to the nucleus during neuronal migration (Tanaka *et al.*, 2004; Kardon and Vale, 2009).

This article was published online ahead of print in MBoC in Press (http://www.molbiolcell.org/cgi/doi/10.1091/mbc.E12-07-0558) on October 24, 2012.

The authors made the following contributions to this work. Conceived and designed experiments: J.N.J. and L.A.L. Execution of experiments: J.N.J. Antibody production and purification: M.S. and B.R. *Drosophila* experiments: P.S. and H.Z.-S. Intellectual contributions: E.L. Manuscript preparation: J.N.J. and L.A.L.

Address correspondence to: Laura Lee (laura.a.lee@vanderbilt.edu).

Abbreviations used: Ab, antibody; *asun*, *asunder*; ASUN, Asunder; BICD2, Bicaudal D2; CENP-F, centromere protein F; CHY, mCherry; dASUN, *Drosophila* Asunder; DHC, dynein heavy chain; DIC, dynein intermediate chain; DMN, dynamitin; HA, hemagglutinin; hASUN, human Asunder; LIS1, lissencephaly 1; mASUN, mouse Asunder; NE, nuclear envelope; NEBD, nuclear envelope breakdown; NPC, nuclear pore complex; NT, nontargeting; PH3, phosphorylated histone H3; RPE, retinal pigment epithelial.

A dynein subpopulation stably anchored to the nuclear envelope (NE) at the G2/M transition is essential for proper nucleus–centrosome coupling in multiple systems (Malone *et al.*, 2003; Anderson *et al.*, 2009; Splinter *et al.*, 2010; Bolhy *et al.*, 2011). Minus end–directed movement of anchored dynein motors along astral microtubules has been hypothesized to draw centrosomes toward the nuclear surface to facilitate their attachment to the NE before nuclear envelope breakdown (NEBD; Burgess and Knight, 2004). This anchored pool of dynein has also been implicated in the process of NEBD (Beaudouin *et al.*, 2002; Salina *et al.*, 2002).

Although promotion of nucleus–centrosome coupling is a dynein-dependent function that is evolutionarily conserved, the exact molecular mechanisms appear to vary (Salina *et al.*, 2002). Dynein is anchored to the nuclear surface via KASH and SUN domain–containing proteins in *Caenorhabditis elegans* embryogenesis and during neuronal migration in mice (Malone *et al.*, 2003; Zhang *et al.*, 2009). In a cultured mammalian cell line (HeLa), at least two distinct pathways are required to ensure proper execution of this critical event. These pathways both employ nuclear pore complex (NPC) interactions to anchor dynein motors to the nuclear surface. The first pathway uses RanBP2, a nucleoporin that associates with the cytoplasmic face of NPCs, as the docking site for Bicaudal D2 (BICD2; Splinter *et al.*, 2010). BICD2, directly bound to dynein, moves in a minus-end direction toward the nuclear surface just before the G2/M transition, thereby anchoring dynein at the NE. The second pathway uses another nucleoporin, Nup133, as a docking site for centromere protein F (CENP-F; Bolhy *et al.*, 2011). Before G2/M, CENP-F directly binds dynein-bound NudE/EL; CENP-F then simultaneously binds Nup133 to anchor dynein, NudE/EL, and ultimately the centrosomes to the NE.

We previously identified *asunder* (*asun*; formerly known as *Mat89Bb*) as an essential regulator of dynein localization during *Drosophila* spermatogenesis (Anderson *et al.*, 2009). Spermatocytes of *asun* mutant testes arrest at prophase of meiosis I with centrosomes unattached to the nucleus. *asun* spermatocytes that progress beyond this arrest exhibit defects in meiotic spindle assembly, chromosome segregation, and cytokinesis. The severe loss of perinuclear dynein in *asun* spermatocytes is the likely basis for this constellation of defects. Our studies revealed that *Drosophila* ASUN (dASUN) plays a key role in recruiting dynein to the nuclear surface at G2/M, a critical step in establishing nucleus–centrosome coupling and fidelity of meiotic divisions.

The human homologue of *asun* (also known as *GCT1* or *C12ORF11*) was originally identified in a screen for genes up-regulated in testicular seminomas (Bourdon *et al.*, 2002). Whereas expression of *Drosophila asun* is limited to male and female germline cells, transcripts of the mouse homologue were detected in both germlines and all somatic cells surveyed (Stebbings *et al.*, 1998; Bourdon *et al.*, 2002). These findings suggested that Asunder (ASUN) might play a broader role in mammals.

To further investigate the mechanism by which ASUN regulates dynein, we examined the function of the human homologue of ASUN (hASUN) in this study. We find that, like BICD2 and CENP-F, hASUN is required in cultured cells for enrichment of dynein on the nuclear surface at the onset of mitosis. hASUN depletion leads to mitotic defects, which are likely secondary to failure of dynein localization. We present a model in which hASUN acts via a mechanism distinct from that of BICD2 and CENP-F to promote dynein recruitment to the nuclear surface at G2/M, a critical step to establishing nucleus–centrosome coupling and fidelity of mitotic divisions.

RESULTS

Mammalian ASUN can functionally replace dASUN during spermatogenesis

The predicted hASUN and mouse ASUN (mASUN) proteins are 95% identical and 97% similar to each other; comparison of the predicted mammalian and *Drosophila* ASUN proteins revealed that they are 43% identical and 64% similar. We sought to determine whether a mammalian form of ASUN could functionally replace dASUN in vivo. Using the *Drosophila* model system, we established transgenic lines expressing mCherry-tagged mASUN (CHY-mASUN) exclusively in the male germline (Figure 1A). We found that the presence of a single copy of the CHY-mASUN transgene significantly increased the percentage of $asun^{f02815}$ males (hypomorphic allele) that produced adult progeny (Figure 1B; Anderson *et al.*, 2009). We also observed a significant increase in the number of adult progeny produced per fertile male, albeit not to the level of wild-type controls (Figure 1C). We previously reported that germline expression of CHY-tagged dASUN fully rescued the sterility of *asun* males; the partial rescue obtained by germline expression of the mouse homologue might be due to the relatively low level of expression of this fusion protein in the fly testes (Figure 1A; Anderson *et al.*, 2009).

We previously identified a critical role for dASUN in recruitment of dynein motors to the nuclear surface and nucleus–centrosome coupling in *Drosophila* male germline cells (Anderson *et al.*, 2009). We next asked whether a mammalian form of ASUN could similarly regulate these events. The severe reduction of perinuclear dynein heavy chain (DHC) that is a hallmark feature of *asun* G2 spermatocytes and immature spermatids was almost fully restored to wild-type levels by transgenic CHY-mASUN expression (Figure 1, D–H). We also observed a significant increase in the degree of nucleus–centrosome coupling at prophase in *asun* spermatocytes harboring the CHY-mASUN transgene (Figure 1, I and J). Together these findings reveal that mASUN can functionally replace its *Drosophila* homologue in vivo to regulate dynein localization during spermatogenesis and suggest that the molecular function of ASUN is conserved across phyla.

hASUN is required for dynein anchoring to the NE at prophase

On the basis of the role of dASUN during male meiosis and the broader expression pattern of mASUN, we reasoned that vertebrate homologues of ASUN might promote dynein recruitment to the NE of somatic cells at the onset of mitosis. To test this hypothesis, we performed small interfering RNA (siRNA)–mediated knockdown of hASUN in HeLa cells. We confirmed that ASUN was efficiently depleted from cells by immunoblotting with antipeptide antibodies (M-hASUN antibody [Ab] and C-hASUN Ab) directed against distinct epitopes in the C-terminal region of hASUN (Supplemental Figure S1A). siRNA-treated cells were briefly incubated with nocodazole to enhance perinuclear localization of dynein–dynactin complexes and accessory proteins before fixation and immunostaining for dynein intermediate chain (DIC; Beswick *et al.*, 2006; Hebbar *et al.*, 2008; Splinter *et al.*, 2010; Bolhy *et al.*, 2011). We found that ~91% of NT-siRNA (nontargeting control) prophase cells showed strong perinuclear dynein staining (Figure 2, A and D–F). After hASUN knockdown, however, only ~30% of cells exhibited this pattern; instead, the majority of prophase cells displayed diffuse localization of dynein in the cytoplasm (Figure 2, B and D–F). Using a second independent hASUN-siRNA sequence that efficiently depleted ASUN from cells, we observed a similar reduction in the percentage of prophase cells with perinuclear dynein (Supplemental Figure S1, B–D).

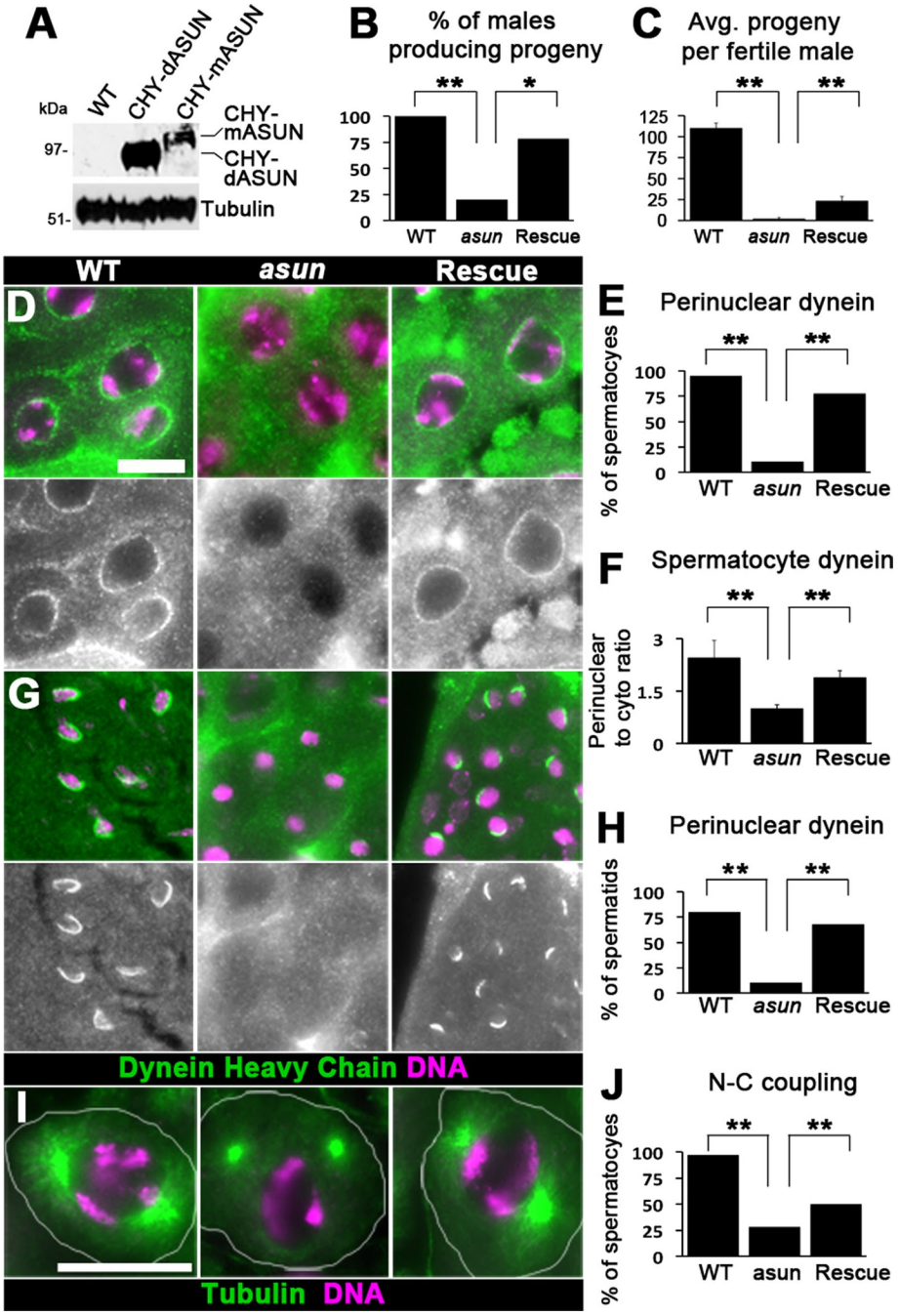

FIGURE 1: mASUN partially rescues spermatogenesis defects of *Drosophila asun* mutants. (A) Anti-CHY immunoblot of testes extracts from *Drosophila* wild-type (WT) males with or without germline expression of CHY-dASUN or CHY-mASUN; a relatively low expression level of a fusion protein of the expected size was observed for the latter. Tubulin was used as loading control. (B, C) Male fertility assays. "Rescue" indicates *asun* males with germline expression of CHY-mASUN, which increased the percentage of *asun* males producing progeny (B) and the average number of progeny per fertile male (C). (D–H) Germline CHY-mASUN expression restored perinuclear dynein in *asun* primary spermatocytes and spermatids. (D–F) Representative G2 spermatocytes stained for DHC and DNA are shown (D) with bar graphs depicting percentages of spermatocytes exhibiting perinuclear DHC (E) and average ratios of perinuclear to diffusely cytoplasmic DHC signal intensities (F). (G, H) Representative immature spermatids stained for DHC and DNA are shown (G) with bar graph depicting percentages of spermatids exhibiting perinuclear DHC (H). (I, J) Germline CHY-mASUN expression restored nucleus–centrosome coupling in *asun* primary spermatocytes. (I) Prophase I spermatocytes stained for β-tubulin and DNA. (J) Quantification of nucleus–centrosome coupling in prophase spermatocytes. $^{**}p < 0.0001$, $^{*}p < 0.001$. Scale bars, 50 μm.

We considered the possibility that hASUN might function to destabilize microtubules; in that case, down-regulation of hASUN could inhibit nocodazole-induced depolymerization of microtubules, thereby blocking access of dynein to the NE. We performed immunostaining experiments to assess whether microtubules undergo a normal degree of nocodazole-induced depolymerization after loss of hASUN. We observed essentially identical tubulin staining patterns for NT-siRNA versus hASUN-siRNA cells in response to nocodazole treatment, suggesting that the lack of perinuclear dynein observed in hASUN-siRNA cells is not secondary to gross alterations of the microtubule network (Supplemental Figure S2).

To further confirm that loss of perinuclear dynein in hASUN-siRNA HeLa cells was due to depletion of endogenous hASUN, we performed a rescue experiment by transiently expressing CHY-tagged dASUN (refractory to hASUN siRNA). CHY-dASUN restored perinuclear dynein in hASUN-siRNA prophase cells to levels similar to that of control cells (Figure 2, C–F). These results confirmed that loss of perinuclear dynein in hASUN-siRNA cells was specifically caused by hASUN depletion and demonstrated that dASUN can replace its human homologue to promote dynein recruitment to the NE at prophase.

We considered an alternative possibility that hASUN is required for stability of dynein–dynactin complexes rather than to promote their enrichment on the NE. Depletion of individual dynein–dynactin components can destabilize other subunits of these complexes (Schroer, 2004; Mische *et al.*, 2008). We immunoblotted for DIC and dynamitin (DMN; dynactin subunit) in extracts of HeLa cells after hASUN knockdown and found no changes in their cellular levels (Supplemental Figure S3A). We also performed sucrose density gradient analysis to assess whether dynein complexes remained intact after hASUN knockdown and found no change in migration profiles (Supplemental Figure S3B). Taken together, these data suggest that hASUN is not required to maintain the integrity of dynein–dynactin complexes.

hASUN is required for proper coupling of centrosomes to the NE at prophase

Perinuclear dynein is essential for proper tethering of centrosomes to the NE at G2/M (Splinter *et al.*, 2010; Tanenbaum *et al.*, 2010; Bolhy *et al.*, 2011). On the basis of the loss of perinuclear dynein we observed in hASUN-siRNA HeLa cells at prophase, we predicted that nucleus–centrosome coupling defects would ensue. We used the human osteosarcoma U2OS cell line for these

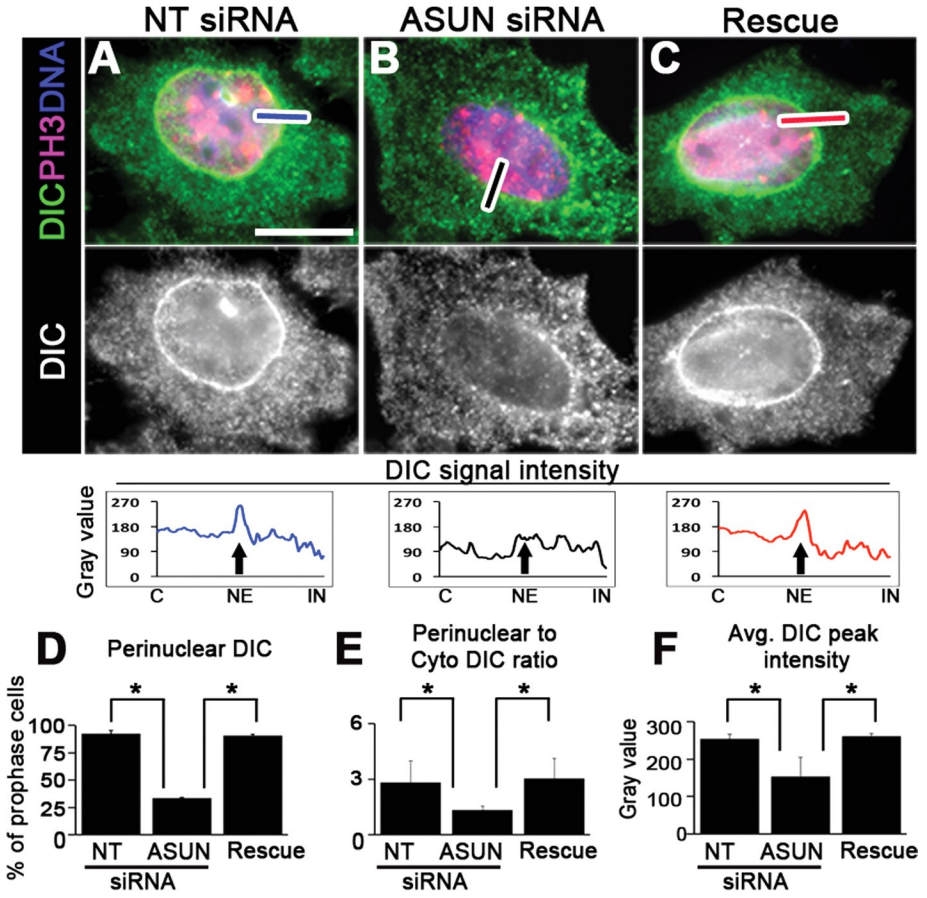

FIGURE 2: hASUN is required for localization of dynein to the NE at mitotic entry. (A–C) HeLa cells were transfected with NT siRNA, hASUN siRNA, or hASUN siRNA plus a CHY-dASUN expression construct ("Rescue"). After nocodazole treatment, cells were fixed and stained for DIC, PH3, and DNA. Both the percentage of prophase cells with perinuclear DIC and the ratio of perinuclear to cytoplasmic DIC signal intensity were reduced by hASUN knockdown (compare B to A); CHY-dASUN expression rescued these defects (C). Note that CHY-dASUN cannot be visualized in C because its signal intensity was much weaker than that of PH3 (visualized with Cy3-conjugated secondary antibodies). (D–F) Quantification of dynein localization defects in hASUN-siRNA cells. Representative line scans (corresponding to blue, black, and red lines in A– C, respectively) of DIC intensity centered at the NE (marked by arrows) are shown below each micrograph with average peak intensities plotted in F. C, cytoplasmic; IN, intranuclear. *$p < 0.0001$. Scale bars, 20 μm.

studies. Owing to the relatively decreased density of the microtubule network in these cells, centrosomes undergo a more dramatic migration from the nucleus to the cortex at interphase and back to the nuclear surface at G2/M (Akhmanova and Hammer, 2010).

We found that ~19% of hASUN-siRNA U2OS cells exhibited loss of coupling of one or both centrosomes to the NE at prophase, compared with a baseline rate of ~4% in control cells (Figure 3, A–E, and Supplemental Figure S1A). We measured an average distance of ~8 μm between the nucleus and centrosomes in hASUN-siRNA cells, compared with a baseline distance of ~3 μm in control cells (Figure 3F). These data indicate that hASUN is required for normal linkage of centrosomes to the NE during prophase, and they further demonstrate evolutionary conservation of function of ASUN homologues.

hASUN is required for proper spindle formation and fidelity of mitotic divisions

The evidence suggests that the perinuclear pool of dynein mediating nucleus–centrosome coupling at G2/M is also required for the fidelity of subsequent mitotic events (Splinter *et al.*, 2010; Tanenbaum *et al.*, 2010). If centrosomes are improperly coupled to the NE at prophase, their separation to prospective poles before NEBD may be random, leaving room for errors in mitotic spindle assembly and chromosome segregation (Tanenbaum *et al.*, 2010). Given our identification of a role for hASUN in dynein recruitment and centrosomal tethering to the NE at mitotic prophase, we assessed whether loss of hASUN in HeLa cells would induce downstream mitotic defects.

We tested the capacity of HeLa cells to form normal bipolar spindles after hASUN knockdown. To enrich for cells with mitotic spindles, we treated siRNA-transfected cells with a Cdk1 inhibitor (RO-3306) and released them into media containing a proteasome inhibitor (Vassilev, 2006). We found that ~35% of hASUN-siRNA metaphase cells exhibited mitotic spindle defects, including scattered chromosomes and broadened spindles; these phenotypes, which were seen in ~9% of NT-siRNA metaphase cells, were fully rescued by CHY-dASUN expression (Figure 4, A–C and G). Similarly, in the absence of drug treatment, we observed a nearly fourfold higher incidence of spindle defects in hASUN-siRNA metaphase cells compared with control cells (Supplemental Figure S4A). We found that hASUN-siRNA cells concomitantly exhibited a ~50% increase in the mitotic index (12.1 vs. 8.1% for control cells), suggesting that loss of hASUN can lead to a mild delay in progression through mitosis (Supplemental Figure S4B).

We also assessed DNA content after loss of hASUN by microscopic examination of DNA-stained HeLa cells. We previously noted the presence of multinucleated HeLa cells after hASUN down-regulation; this phenotype, however, was not quantified or further characterized (Lee *et al.*, 2005). To quantify the multinucleation phenotype, we scored cells only if they contained more than two nuclei due to the common occurrence of binucleation in control HeLa cells. We found that ~37% of hASUN-siRNA cells were multinucleated (typically containing three nuclei), compared with ~9% of control cells, and this defect was fully rescued by CHY-dASUN expression (Figure 4, D–F and H). Furthermore, loss of hASUN caused an even more severe degree of multinucleation: ~6% of hASUN-siRNA cells contained more than four nuclei, which we never observed in control cells (12 of 177 and 0 of 165 cells, respectively; Figure 4F). Using a second independent siRNA sequence, we also observed multinucleation of HeLa cells after hASUN knockdown (Supplemental Figure S1E).

A common cause of multinucleation involves successful completion of chromosome segregation during mitosis, followed by a lack of cell division; increased centriole number is another indicator of cytokinesis failure (Godin and Humbert, 2011; Lacroix and Maddox, 2012). In addition to multinucleation, we observed supernumerary

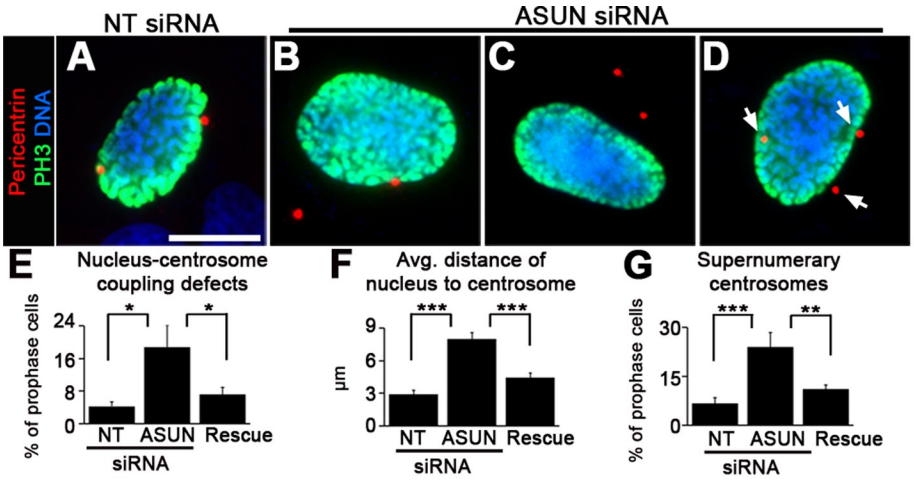

FIGURE 3: hASUN is required for recruitment of centrosomes to the NE at mitotic entry. (A–D) U2OS cells were transfected with NT or hASUN siRNA, fixed, and stained for pericentrin (centrosomal marker), PH3, and DNA. hASUN knockdown yielded an increased percentage of prophase cells with loss of coupling of one (B) or both (C) centrosomes to the NE compared with control cells (A) as well as supernumerary centrosomes (arrows in D). (E–G) Quantification of centrosome defects in hASUN-siRNA cells. Expression of CHY-dASUN in hASUN-siRNA cells ("Rescue") corrected these defects. ***$p < 0.0001$, **$p < 0.005$, *$p < 0.02$. Scale bar, 20 µm.

centrosomes in ~24% of prophase cells after hASUN knockdown, compared with ~5% of control cells; this defect was corrected by expression of CHY-dASUN (Figure 3, D and G). Our data are consistent with a possible role for hAUN in mitotic events downstream of nucleus–centrosome coupling: proper spindle formation and execution of cytokinesis.

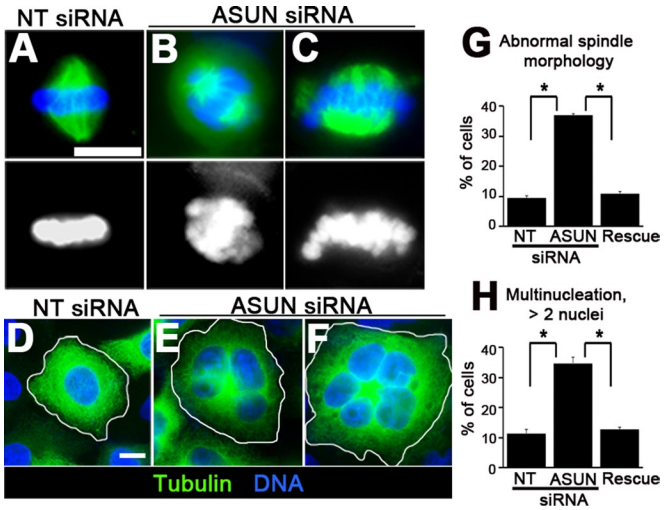

FIGURE 4: Loss of hASUN causes mitotic spindle defects and multinucleation. (A–F) HeLa cells were transfected with NT or hASUN siRNA, fixed, and stained for tubulin and DNA. (A–C) Mitotic spindles. To enrich for mitotic spindles, cells were arrested in metaphase before fixation. NT-siRNA cells had bipolar spindles with tight alignment of chromosomes at metaphase (A). hASUN-siRNA cells had an increased percentage of abnormal spindles with defects such as scattering of chromosomes along spindles (B) and broadened spindles (C). (D–F) Interphase cells. An increased percentage of hASUN-siRNA cells (E, F) were multinucleated (more than two nuclei) compared with NT-siRNA cells (D). We occasionally observed a more severe degree of multinucleation (more than four nuclei) in hASUN-siRNA cells (F). (G, H) Quantification of spindle morphology defects (G) and multinucleation (H) in hASUN-siRNA cells. Expression of CHY-dASUN in hASUN-siRNA cells ("Rescue") corrected these defects. * $p < 0.0001$. Scale bars, 20 µm.

hASUN is required for dynein anchoring to the NE at prophase in nontransformed cells

To confirm that the observed loss of NE-bound dynein after knockdown of hASUN is independent of the transformed nature of HeLa cells, we performed a similar analysis using human retinal pigment epithelial (RPE) cells, which are nontransformed. We detected strong perinuclear localization of dynein after nocodazole treatment in 59% of control RPE cells; in contrast, we observed this staining pattern in only 12% of cells after knockdown of hASUN (Figure 5, A–D). We observed an increased frequency of multinucleation in RPE cells after hASUN knockdown, possibly due to downstream mitotic defects caused by loss of perinuclear dynein: ~35% of hASUN-siRNA cells had more than one nucleus, compared with ~10% of control cells (Figure 5, E–G). These data suggest that the role of hASUN in regulating recruitment of dynein to the nuclear surface is not limited to transformed cells.

hASUN is cytoplasmic at G2/M

We previously reported that a tagged form of dASUN exhibited a meiotic stage–specific localization pattern in *Drosophila* spermatocytes: intranuclear in early G2 and appearing in the cytoplasm in late G2, coincident with dynein recruitment to the nuclear surface (Anderson *et al.*, 2009). Tagged versions of dASUN and hASUN co-expressed in HeLa cells exhibited similar localization patterns during mitosis (Anderson *et al.*, 2009).

To further understand the mechanism by which ASUN controls dynein localization at G2/M, we sought to determine the localization pattern of the endogenous protein in cultured human cells during prophase. Using C-hASUN Ab for immunostaining of HeLa cells, we found endogenous hASUN to be localized to the cytoplasm in ~98% of prophase cells (85 of 87 cells; Figure 6A). We used the following criteria to identify prophase cells: phosphorylated histone (PH3)-positive DNA and intact NE.

To further confirm that this localization pattern reflects that of endogenous hASUN, we transfected HeLa cells with either control or hASUN siRNA, followed by immunostaining with C-hASUN Ab. The hASUN signal present in control cells was lost in hASUN-siRNA cells, demonstrating specificity (Figure 6, B and C). We confirmed these results with a second hASUN-siRNA sequence (Supplemental Figure S1C). We found that Myc-tagged mASUN transiently expressed in HeLa cells tightly colocalized with endogenous hASUN, indicating a conserved localization pattern of the human and mouse homologues, which are ~95% identical at the amino acid level (Figure 6D).

Two dynein-recruiting proteins, BICD2 and CENP-F, have recently been reported to bind NPCs at prophase via direct interactions with the NPC components RanBP2 and Nup133, respectively (Splinter *et al.*, 2010; Bolhy *et al.*, 2011). Owing to their similar functions in recruiting dynein complexes to the NE, we considered

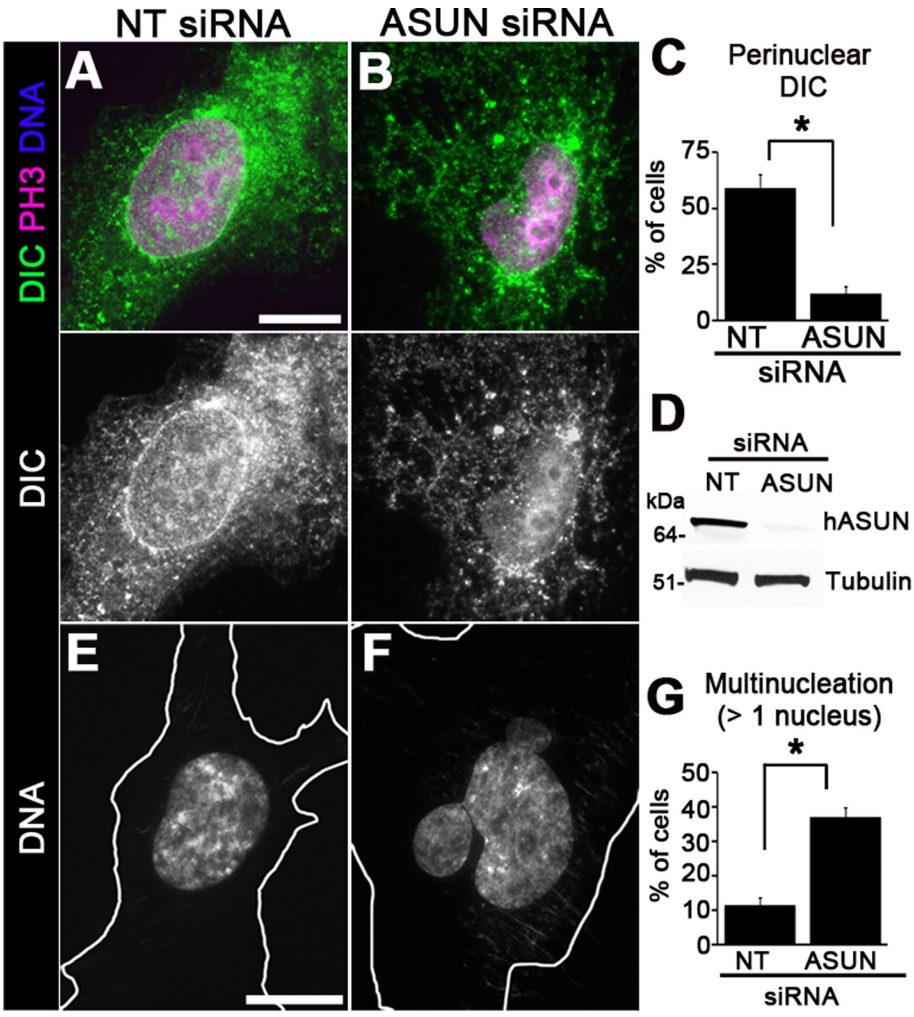

FIGURE 5: Loss of hASUN causes reduction of perinuclear dynein and multinucleation in nontransformed cells. (A–C) Dynein localization defects in hASUN-siRNA RPE cells. RPE cells were transfected with NT or hASUN siRNA. After nocodazole treatment, cells were fixed and stained for DIC, PH3, and DNA. The percentage of prophase cells with perinuclear DIC was reduced after hASUN knockdown (B) compared with control cells (A; quantified in C). (D) Immunoblotting of lysates confirmed down-regulation of hASUN. Tubulin was used as loading control. (E–G) A higher percentage of hASUN-siRNA RPE cells (F) were multinucleated (more than one nucleus per cell) compared with control cells (E; quantified in G). *$p < 0.0005$. Scale bars, 20 μm.

the possibility that hASUN might also bind to NPCs at prophase. We observed minimal colocalization, however, of endogenous hASUN and a marker for NPCs in costained cells (Figure 6E).

hASUN interacts with the dynein adaptor LIS1

We recently demonstrated a strong genetic interaction between *Drosophila asun* and *Lis-1*, coimmunoprecipitation and colocalization of dASUN and *Drosophila* LIS-1 proteins in cultured cells, and dependence of LIS-1 localization on dASUN during spermatogenesis (Sitaram *et al.*, 2012). On the basis of these findings, we considered the possibility that this interaction might be conserved between the mammalian homologues.

We showed coimmunoprecipitation of Myc-tagged mASUN and hemagglutinin (HA)-tagged human LIS1 after their coexpression in HEK293 cells, suggesting that these proteins exist within a complex; the capacity of these two proteins to coimmunoprecipitate was maintained when the affinity tags were switched (Figure 7, A and B, and Supplemental Figure S5). We also demonstrated coimmunoprecipitation of human LIS1 and *Drosophila* ASUN proteins, further indicating evolutionary conservation of this interaction (Supplemental Figure S6). In further support of these data, we found that CHY-LIS1 colocalizes with endogenous hASUN in the perinuclear region of ~70% of nocodazole-treated HeLa cells (Figure 7, C and E). Line scans confirmed that hASUN and CHY-LIS1 have overlapping staining patterns, although tight colocalization was not consistently observed (Figure 7D). Despite the interaction observed between ASUN and LIS1, we did not detect coimmunoprecipitation of ASUN and dynein–dynactin subunits (Supplemental Figure S7A).

To further explore the nature of the relationship between ASUN and LIS1, we tested whether hASUN is required for perinuclear enrichment of LIS1 at G2/M. After nocodazole treatment, perinuclear CHY-LIS1 was detected in <25% of cells with loss of hASUN, compared with ~80% of control cells (Figure 7, F and G). Immunoblot analysis revealed no change in CHY-LIS1 levels after hASUN knockdown, suggesting that ASUN is not required to maintain steady-state levels of LIS1 within cells (Figure 7H). These data are consistent with a model in which hASUN acts via LIS1 to recruit dynein complexes to the NE at prophase. The localization of ASUN at G2/M, however, was not dependent on LIS1 (Figure 7, I and J, and Supplemental Figure S8).

hASUN, BICD2, and CENP-F localize independently of each other at prophase

Two pathways, BICD2–RanBP2 and NudE/EL–CENP-F–Nup133, have been described that appear to operate independently to anchor dynein to the NE and facilitate proper positioning of centrosomes at the G2/M transition (Splinter *et al.*, 2010; Bolhy *et al.*, 2011). We confirmed that BICD2 and CENP-F colocalize to the NE of prophase HeLa cells as we would predict on the basis of independent reports of their localization patterns (Figure 8A; Splinter *et al.*, 2010; Bolhy *et al.*, 2011). As expected from our demonstration that the hASUN immunostaining pattern excludes the NE, we observed essentially no overlap of endogenous hASUN and GFP-BICD2 signals (Figure 8B). Furthermore, we observed no coimmunoprecipitation from cell lysates of ASUN with either BICD2 or CENP-F (Supplemental Figure S7, B and C).

We asked whether knockdown of hASUN, BICD2, or CENP-F in HeLa cells would globally disrupt the structure of NPCs in such a way that docking of dynein motors to the nuclear surface might be blocked. In hASUN-siRNA cells exhibiting loss of dynein at the NE, nuclear pore morphology as assessed by immunostaining for an NPC marker resembled that of control cells; similarly, depletion of BICD2 or CENP-F caused loss of dynein at the NE without grossly disrupting NPCs (Figure 8C and Supplemental Figure S9).

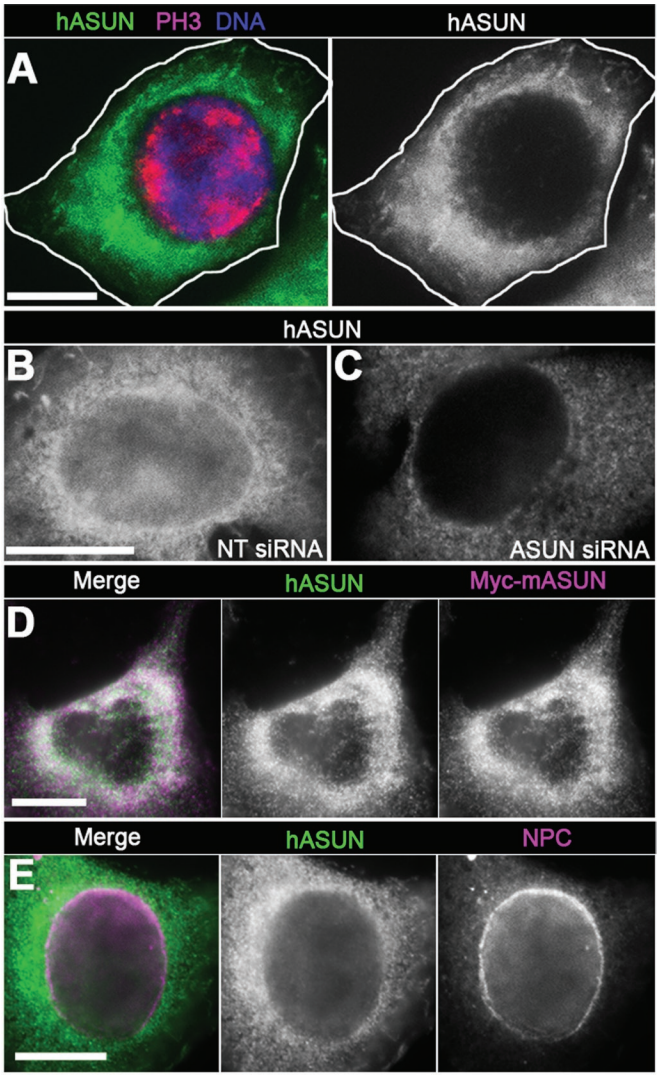

FIGURE 6: Subcellular localization of ASUN. HeLa cells were immunostained for endogenous hASUN using antipeptide antibodies (C-hASUN Ab). (A) PH3 costaining revealed endogenous hASUN localizes to the cytoplasm of prophase cells. (B, C) The hASUN signal of NT-siRNA cells (B) was lost in hASUN-siRNA cells (C), thereby demonstrating specificity. (D) Colocalization of endogenous hASUN and transiently expressed Myc-tagged mASUN. (E) Costaining of endogenous hASUN revealed no significant overlap with the NPC marker Mab414. Scale bars, 20 μm.

We next assessed whether hASUN, BICD2, or CENP-F is localized within HeLa cells in an interdependent manner (Figure 8D). We observed no change in the cytoplasmic localization pattern of hASUN after depletion of BICD2 or CENP-F. Conversely, BICD2 and CENP-F localized normally to the NE in hASUN-siRNA cells. We confirmed the previous observations of Bolhy *et al.* (2011) that BICD2 and CENP-F are not reciprocally required for their anchoring to the NE. Taken together, these data suggest that hASUN, BICD2, and CENP-F localize independently of each other at G2/M.

It was previously reported that inhibition of dynein function (via dynein antibody injection or dynactin subunit overexpression) does not disrupt the recruitment of BICD2 or CENP-F to the NE at G2/M (Splinter *et al.*, 2010; Bolhy *et al.*, 2011). We used siRNA-mediated knockdown to test whether the dynein adaptor LIS1 is required to properly localize BICD2 or CENP-F. We observed no alteration in the localization patterns of BICD2 or CENP-F in prophase HeLa cells, providing further confirmation that functional dynein motors are not reciprocally required to recruit these proteins to the NE (Supplemental Figure S10).

hASUN, BICD2, and CENP-F cooperatively regulate dynein recruitment to the NE at prophase

We investigated possible cross-talk between hASUN, BICD2, and CENP-F in their regulation of dynein recruitment to the NE and nucleus–centrosome coupling at prophase. After knockdown of these three proteins, either individually or in combination, we assessed perinuclear dynein localization in nocodazole-treated HeLa cells and average nucleus–centrosome distances in U2OS cells (Figure 8, E and F). We did not observe additive or synergistic effects on these phenotypes in the double- or triple-knockdown cells. Bolhy *et al.* (2011) reported similar findings for the average nucleus–centrosome distances in U2OS cells with double knockdown of BICD2 and CENP-F. These observations suggest that hASUN, BICD2, and CENP-F operate via distinct molecular mechanisms but converge to regulate dynein localization and centrosomal tethering to the NE in prophase.

DISCUSSION

Proposed mechanism for hASUN-mediated recruitment of dynein to the NE during mitotic prophase

Two recent studies advanced our understanding of the mechanisms underlying the recruitment of dynein motors to the NE of cultured human cells at the onset of mitosis (Splinter *et al.*, 2010; Bolhy *et al.*, 2011). BICD2–RanBP2 and NudE/EL–CENP-F–Nup133 were identified as separate cassettes of proteins that provide sites to anchor dynein to the NE. We report here our findings that hASUN is a third protein required for this critical event in cultured cells. In contrast to the BICD2 and CENP-F cassettes, however, which can bind directly to components of dynein complexes, our data suggest that hASUN regulates the localization of dynein in an indirect manner via LIS1, an accessory protein of the motor. Another distinction is that BICD2 and CENP-F localize to NPCs within the NE, whereas hASUN localizes to the cytoplasm with exclusion of the NE.

We propose a model in which hASUN works in a manner distinct from that of BICD2 and CENP-F to mediate dynein recruitment to the NE at G2/M, a critical event required for nucleus–centrosome coupling before NEBD and faithful execution of mitotic divisions. Our data lead us to hypothesize that cytoplasmic hASUN transiently interacts with LIS1, which is bound to dynein heavy chains, to promote the enrichment and/or proper orientation of dynein complexes in the vicinity of the nuclear surface at G2/M. The BICD2–RanBP2 and NudE/EL–CENP-F–Nup133 cassettes then capture and stably anchor dynein complexes to NPCs. In the absence of hASUN, BICD2 and CENP-F are not sufficient to carry out the early steps in the process of dynein recruitment to the NE at G2/M; similarly, when either BICD2 or CENP-F is depleted from cells, hASUN can promote the enrichment/orientation of dynein complexes near the nuclear surface, but the complexes do not become stably anchored to the NE.

Why are so many factors required to carry out this important cellular process? A network of proteins might be required to move and properly orient dynein complexes at G2/M, given their large size and multisubunit composition. NudE, in addition to directly interacting with dynein motors, facilitates the interaction between LIS1 and dynein, suggesting that both ASUN and the NudE/EL–CENP-F–Nup133 cassette might converge on dynein through

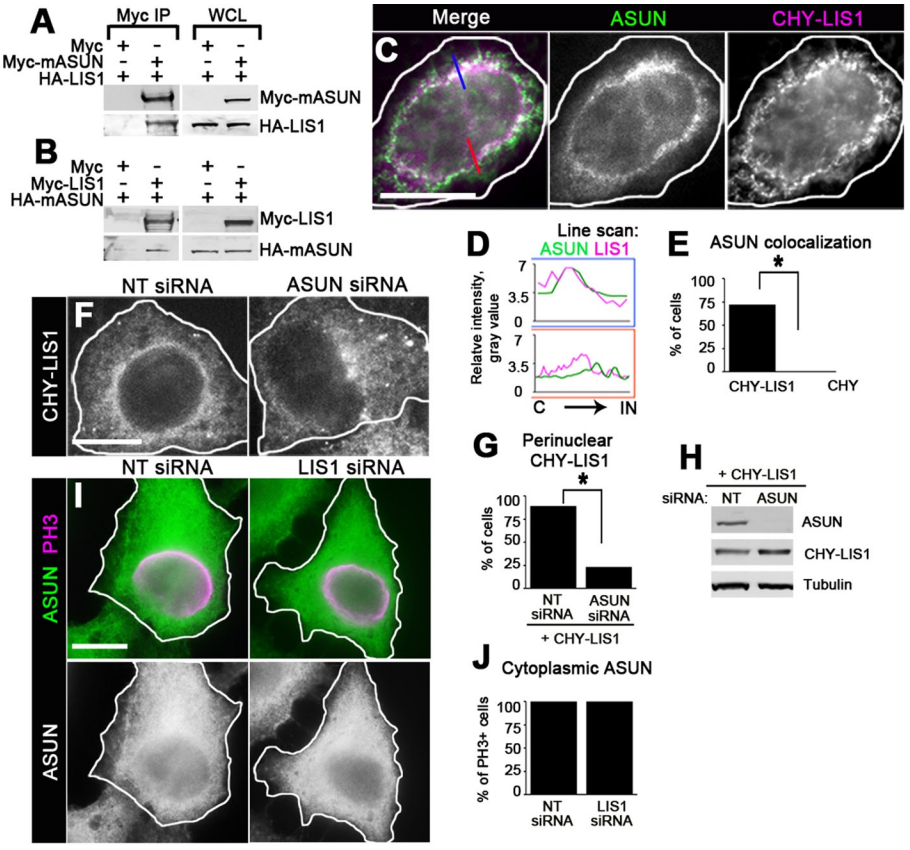

FIGURE 7: Interactions between ASUN and LIS1. (A, B) Coimmunoprecipitation experiments. (A, B) Lysates of HEK293 cells coexpressing the indicated tagged versions of mASUN and human LIS1 were used for Myc immunoprecipitation. Immunoblots of whole-cell lysates (WCL) and Myc immunoprecipitates (IP) were probed with HA and Myc antibodies. Representative blots are shown. (C–E) Overlapping localizations of hASUN and CHY-LIS1. Transfected HeLa cells expressing CHY-LIS1 were treated with nocodazole, fixed, and stained for hASUN. (C) Representative cell with partial overlap of hASUN and CHY-LIS1 in the perinuclear region is shown. (D) Line scans centered at the NE (corresponding to blue and red lines in D) confirmed colocalization of hASUN and CHY-LIS1 in some but not all areas. C, cytoplasmic; IN, intranuclear. (E) Quantification of overlap of perinuclear CHY-LIS1 (but not CHY) and hASUN in a majority of transfected cells. (F–H) Perinuclear localization of CHY-LIS1 is hASUN dependent. HeLa cells cotransfected with NT or hASUN siRNA plus CHY-LIS1 expression construct were treated with nocodazole and fixed. (F) Representative hASUN-siRNA cell with loss of perinuclear CHY-LIS1 compared with control. (G) Quantification of the loss of perinuclear CHY-LIS1 after hASUN knockdown. (H) Immunoblotting revealed no change in steady-state levels of CHY-LIS1 protein after hASUN knockdown. Tubulin was used as loading control. (I, J) ASUN localization at G2/M is independent of LIS1. HeLa cells transfected with NT or LIS1 siRNA were stained for PH3 and ASUN. (I) NT-siRNA and LIS1-siRNA cells showed comparable ASUN staining patterns. (J) Quantification of cytoplasmic ASUN localization in PH3+ cells after LIS1 knockdown. *$p < 0.0001$. Scale bars, 20 μm.

LIS1 at the onset of mitosis (McKenney *et al.*, 2010). It will be interesting to test in future experiments whether ASUN plays a role in promoting the interaction between CENP-F tethered to the NE and cytoplasmic NudE/EL–LIS1–dynein complexes at G2/M, a possible mechanism of action that would be consistent with our model.

Meiotic versus mitotic roles of ASUN

Whereas ASUN remained largely uncharacterized in human cells before this study, we previously showed that it has cell cycle and developmental roles in other organisms. In *Drosophila*, dASUN regulates dynein localization and centrosomal tethering to the nucleus during spermatogenesis, and it is required for male fertility (Anderson *et al.*, 2009). In *Xenopus*, we previously reported that the ASUN homologue plays a role during embryonic development (Lee *et al.*, 2005). Down-regulation of ASUN in *Xenopus* embryos via morpholino oligonucleotide injection resulted in disruption of gastrulation and polyploidy; the latter phenotype suggested that ASUN might regulate the mitotic cell cycles of early blastomeres during vertebrate embryogenesis. We also showed conservation of function between *Xenopus* and human ASUN homologues by restoring proper developmental progression in *Xenopus* ASUN morphants via coinjection of mRNA encoding hASUN.

Drosophila asun mutants and HeLa cells depleted of ASUN exhibit strikingly similar disruptions of male meiosis and mitosis, respectively. These shared phenotypes underscore the likelihood that the transformed nature of the HeLa cell line is not responsible for the defects we observed. The reduction of dynein localized to the NE of prophase RPE cells after hASUN knockdown as reported here further validates this conclusion. One difference in the meiotic versus mitotic phenotypes is that *asun* spermatocytes exhibit delayed progression through meiosis, as evidenced by a large increase in the prophase fraction, whereas we report here that hASUN-siRNA HeLa cells have only a slightly increased mitotic index compared with control cells (Anderson *et al.*, 2009). We speculate that dynein localized to the nuclear surface might play a more important role in facilitating nuclear envelope breakdown at the end of prophase in *Drosophila* spermatocytes than in HeLa cells.

In contrast to *Drosophila asun*, which is expressed exclusively in germline tissues, mouse *ASUN* transcripts have been detected in all tissues, both somatic and germline, surveyed in a study by another group (Stebbings *et al.*, 1998; Bourdon *et al.*, 2002). The data we present here indicate that hASUN plays an important role in human somatic cells during mitosis. The human *ASUN* gene is located within a genomic region that is amplified in testicular seminomas, raising the possibility that ASUN may also regulate division of male germline cells in vertebrates as it does in *Drosophila* (Bourdon *et al.*, 2002).

Why might ASUN expression be limited to germline cells in flies? The absence of dASUN expression within somatic cells may be related to the lack of an absolute requirement for centrosomes during most life cycle stages of *Drosophila*. Centrioles, although important for the formation of centrosomes (as well as cilia and flagella), play nonessential roles in development from an embryo to an adult fly, with the exception of early embryogenesis (Basto *et al.*, 2006; Stevens *et al.*, 2007). The process of spermatogenesis in adult male flies is also exceptional in that centrioles are required to form the cilium of spermatocytes and the axoneme of spermatids (Bettencourt-Dias *et al.*, 2005). Centrioles within G2 spermatocytes undergo major changes in

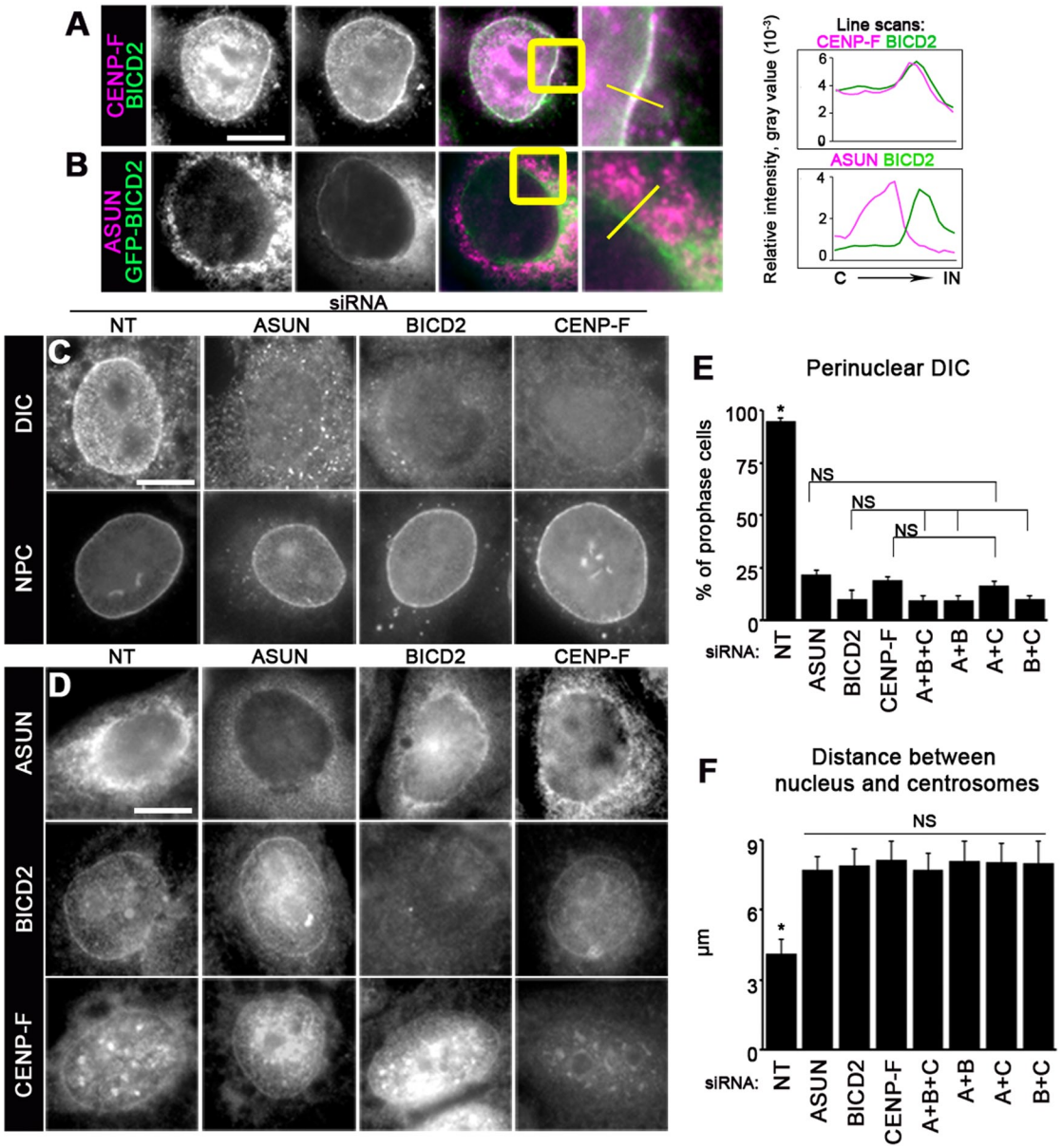

FIGURE 8: Relationship between hASUN, CENP-F, and BICD2 in recruiting dynein and centrosomes to the NE at mitotic entry. (A, B) HeLa cells were nocodazole treated, fixed, and immunostained as indicated. Endogenous CENP-F and BICD2 colocalized on the NE (A), but no colocalization was observed for GFP-BICD2 and endogenous hASUN (B). Higher-magnification views (micrographs on far right) of costained cells in the vicinity of the NE correspond to regions enclosed by yellow boxes. Line scans centered at the NE (corresponding to yellow lines in higher-magnification views) confirmed significant overlap of CENP-F and BICD2 signals but not hASUN and GFP-BICD2 signals. C, cytoplasmic; IN, intranuclear. (C–F) HeLa (C–E) or U2OS (F) cells were transfected with siRNA as indicated to down-regulate hASUN (A), BICD2 (B), and/or CENP-F (C). Transfected cells were nocodazole treated, fixed, and immunostained. (C) Perinuclear DIC was lost after hASUN, BICD2, or CENP-F knockdown without changes in the gross morphology of NPCs. (D) No change in hASUN, BICD2, or CENP-F localization was observed after knockdown of either of the other proteins. (E) Cells were immunostained for PH3, DIC, and DNA. Bar graph displays the percentage of prophase cells with perinuclear DIC for each knockdown condition. (F) Cells were immunostained for PH3, pericentrin, and DNA. Bar graph displays the mean nucleus–centrosome distance for each knockdown condition. *$p < 0.0001$. Scale bars, 20 µm.

their positioning, moving to the cortex during the extensive growth phase to elaborate a cilium and then back toward the nucleus at G2/M; the necessity to reestablish nucleus–centrosome coupling at the time of meiotic entry may impose a stringent requirement for dynein-localizing proteins such as ASUN in these cells (Fuller, 1993). Bicaudal, the *Drosophila* homologue of BICD2, is a potential candidate to cooperate with dASUN in dynein recruitment to the nuclear surface of G2 spermatocytes; our database searches, however, revealed no CENP-F homologues in flies.

Evolved mechanisms for dynein regulation in multicellular organisms

Cytoplasmic dynein, most commonly studied for its roles in trafficking of organelles and directed cell movement, is also required in

multicellular organisms for coordination of mitotic entry and exit (Dujardin *et al.*, 2003). Specifically, dynein promotes the coupling of centrosomes to the NE, has been hypothesized to assist in NEBD, and functions along the mitotic spindle to facilitate chromosome segregation at anaphase (Lippincott-Schwartz, 2002; Dujardin *et al.*, 2003; Tanenbaum *et al.*, 2010). In contrast, only one role for dynein has been identified in budding yeast: proper positioning of the spindle during mitosis (Stuchell-Brereton *et al.*, 2011).

It is interesting to note that none of the three proteins needed for localization of dynein to the NE of prophase HeLa cells (BICD2 and CENP-F as previously reported; hASUN as reported herein) have predicted homologues in either budding or fission yeast. The centrosome-like structure in yeast, known as the spindle pole body, is embedded into the nuclear surface throughout interphase and mitosis in budding yeast (Jaspersen and Winey, 2004). Similarly, in fission yeast, the spindle pole body is tethered to the nuclear surface throughout interphase and will embed at mitosis (Lim *et al.*, 2009). In both cases, dynein is not required for the process of spindle pole body–nucleus embedding (Jaspersen and Winey, 2004; Lim *et al.*, 2009). Thus metazoans appear to have evolved a finely tuned mechanism for regulating the localization of dynein complexes at the onset of mitosis, with at least three proteins required to execute the recruitment and docking of these motors to the NE.

MATERIALS AND METHODS

Drosophila experiments

Flies were maintained at 25°C using standard techniques (Greenspan, 2004). *y w* was obtained from the Bloomington *Drosophila* Stock Center (Indiana University, Bloomington, IN) and used as the "wild-type" stock. The *asun*^{f02815} allele (Exelixis Collection, Harvard Medical School, Boston, MA) and transgenic line with male germline–specific expression of CHY-dASUN were previously described (Anderson *et al.*, 2009). cDNA encoding mASUN (clone details provided later) with an N-terminal CHY tag was subcloned into vector tv3 (a gift from J. Brill, Hospital for Sick Children, Toronto, Canada) for expression of CHY-tagged mASUN under control of the testes-specific β*2-Tubulin* promoter (Wong *et al.*, 2005). Transgenic lines were generated by *P*-element–mediated transformation via embryo injection (Rubin and Spradling, 1982). A single transgene was mapped to the X chromosome and crossed into the *asun*^{f02815} background using standard genetic crosses.

To test male fertility, individual adult males (2 d old) were placed in vials with five wild-type females (2 d old) and allowed to mate for 5 d. The percentage of males producing adult progeny and the average number of live adult progeny produced per fertile male were scored (≥10 males tested per genotype). Statistical analyses were performed using Fisher's exact test (percentage of males producing progeny) or an unpaired Student's *t* test (average number of progeny per fertile male).

Protein extracts were prepared by homogenizing dissected testes from newly eclosed males in SDS sample buffer. The equivalent of eight testes pairs was loaded per lane. After SDS–PAGE, proteins were transferred to nitrocellulose for immunoblotting using standard techniques. Primary antibodies were used as follows: mCherry (1:500, Clontech, Mountain View, CA) and mouse anti–β-tubulin (E7, 1:5000; Developmental Studies Hybridoma Bank, University of Iowa, Iowa City, IA). Horseradish peroxidase (HRP)–conjugated secondary antibodies and chemiluminescence were used to detect primary antibodies.

Live testes cells were prepared for examination by fluorescence microscopy as described previously (Kemphues *et al.*, 1980). Briefly, testes were dissected from newly eclosed adult males, placed in a drop of phosphate-buffered saline (PBS) on a microscopic slide, and gently squashed under a glass coverslip after making a small incision near the stem cell hub. Formaldehyde fixation was performed as described previously (Gunsalus *et al.*, 1995). Briefly, slides of squashed testes were snap-frozen, immersed in 4% formaldehyde (in PBS with 0.1% Triton X-100) for 7 min at –20°C after coverslip removal, and washed three times in PBS. Primary antibodies were used as follows: mouse anti-DHC (P1H4, 1:120; a gift from T. Hays, University of Minnesota, Minneapolis, MN; McGrail and Hays, 1997) and rat anti–α-tubulin (Mca77G, 1:300; Accurate Chemical & Scientific, Westbury, NY). Fixed samples were mounted in PBS with 4′,6-diamidino-2-phenylindole (DAPI) to visualize DNA. Wide-field fluorescence images were obtained using an Eclipse 80i microscope (Nikon, Melville, NY) with Plan-Fluor 40× objective.

In experiments to determine the percentage of late G2 spermatocytes or immature spermatids with perinuclear dynein or the percentage of prophase I spermatocytes with nucleus–centrosome coupling, at least 200 cells were scored per genotype; statistical analyses were performed using Fisher's exact test. To quantify the ratios of perinuclear to diffusely cytoplasmic dynein in late G2 spermatocytes (testes stained for DHC), after image acquisition, the average intensity of the DHC signal within a small rectangular region was sampled near the nuclear surface and in the surrounding cytoplasm using Photoshop (Adobe, San Jose, CA). The ratio of the intensities was determined. At least 30 cells from a minimum of three testes pairs were scored per genotype. Statistical analysis was performed using an unpaired Student's *t* test.

Cell culture and treatments

Cell lines were maintained at 37°C and 5% CO_2 in DMEM (Life Technologies, Carlsbad, CA) containing 10% fetal bovine serum, 1% L-glutamine, 100 μg/ml streptomycin, and 100 U/ml penicillin. U2OS and RPE cells were cultured in antibiotic-free media. Plasmid DNA was transfected into cells using Lipofectamine 2000 (Invitrogen, Carlsbad, CA) or FuGENE HD (Promega, Madison, WI). siRNA duplexes were purchased from Dharmacon (Lafayette, CO). siGENOME NT siRNA#5 was used as negative control. siRNA sequences were designed to target human *ASUN* at its 5′-end (#1: 5′-GGAAAUAGAGGACGAAUAAUU-3′) or its 3′-end (#2: 5′-CAGAAGAGGAAGAACGAAA-3′; *LIS1* (5′-GAGTTGTGCTGATGACAAG-3′; Shu *et al.*, 2004); *CENP-F* (5′-CAGAATCTTAGTAGTCAAGTA-3′; Bolhy *et al.*, 2011); or *BICD2* (5′-GGUGGACUAUGAGGCUAUC-3′; Splinter *et al.*, 2010). hASUN siRNA#1 was used for all experiments in this study unless otherwise indicated. Cells were transfected with siRNA duplexes using DharmaFECT 1 transfection reagent (Dharmacon) in two successive rounds and analyzed 3 d later. Lipofectamine 2000 transfection reagent was used for cotransfection of cells with siRNA and DNA constructs. Where indicated, cells were incubated in 5 μg/ml (16.6 μM) nocodazole (Sigma-Aldrich, St. Louis, MO) for 3 h before fixation to enhance perinuclear localization of dynein. For metaphase arrest, cells were incubated for 16 h in 10 μM RO-3306 (Cdk1 inhibitor; Enzo Life Sciences, Plymouth, PA), followed by incubation for 3 h in 10 μM MG-132 (proteasome inhibitor; Calbiochem, La Jolla, CA). Approximately 80% of cells were arrested in metaphase under these conditions.

Fixation, immunostaining, and microscopy

Cells were fixed in either methanol (5 min at –20°C, followed by washing with Tris-buffered saline [TBS] plus 0.01% Triton X-100) or 4% formaldehyde (20 min at room temperature, followed by 20-min permeabilization step with TBS plus 0.05% Triton X-100). Cells were

blocked in TBS plus 0.01% Triton X-100 and 0.02% BSA before immunostaining. Primary antibodies were used as follows: C-hASUN (1:500), PH3 (Mitosis Marker, 1:1000, Millipore, Billerica, MA; or 1:2000, Abcam, Cambridge, MA), DIC (clone 74.1, 1:500; Abcam), pericentrin centriolar marker (clone 28144, 1:2000; Abcam), c-Myc (9E10, 1:1000), β-tubulin (clone E7, 1:1000; Developmental Studies Hybridoma Bank), CENP-F (clone 14C10 1D8, 1:200; Abcam), BICD2 (1:300; a gift from A. Akhmanova, Erasmus Medical Center, Rotterdam, Netherlands), and NPC marker (Mab414, 1:1000; Abcam). Appropriate secondary antibodies conjugated to Alexa Fluor 488 or Cy3 were used (1:1000; Invitrogen). Cells were mounted in ProLong Gold Antifade Reagent with DAPI (Invitrogen).

Wide-field fluorescence images were obtained using an Eclipse 80i microscope (Nikon) with Plano-Apo 100× objective. Confocal stacks were taken by a Yokogawa QLC-100/CSU-10 spinning disk head (Visitec assembled by Vashaw [Norcross, GA]) attached to a Nikon TE2000E microscope using a CFI PLAN APO VC 100× oil lens/numerical aperture 1.4, with or without 1.5× intermediate magnification, and a back-illuminated Cascade 512B electron-multiplying charge-coupled device camera (Photometrics, Tucson, AZ) driven by IPLab software (Scanalytics, Rockville, MD). A krypton–argon laser (75 mW 488/568; Melles Griot, Albuquerque, NM) with acousto-optic tunable filters was used for two-color excitation. Custom double dichroic mirror and filters (Chroma, Bellows Falls, VT) in a filter wheel (Ludl, Hawthorne, NY) were used in the emission light path. The *Z*-steps (0.2 µm) were driven by a Nikon built-in Z motor.

Line-scan analyses were performed using ImageJ (National Institutes of Health, Bethesda, MD). Ten representative cells were measured per condition; for each cell, 12 line scans distributed equally around the nuclear circumference were obtained. Lines scans presented within figures are 100 pixels in length and are oriented with the cytoplasmic end of each line to the left and the intranuclear end of each line to the right. To quantify the ratios of perinuclear to diffusely cytoplasmic DIC in stained HeLa cells, we sampled the average intensity of the DIC signal within a small rectangular region near the nuclear surface and in the surrounding cytoplasm using ImageJ. The ratio of the intensities was determined. At least 30 cells were scored per condition.

Statistical analyses of experiments reported here were performed using Student's unpaired *t* test unless otherwise noted. Error bars indicate SEM for all bar graphs. All experiments were performed a minimum of three times, with at least 100 cells scored per condition unless otherwise noted.

DNA constructs

cDNA clone LD33046 encoding ASUN was obtained from the *Drosophila* Gene Collection. IMAGE cDNA clones encoding mASUN (#4459471) and human LIS1 (#5786560) were obtained from the American Type Culture Collection (Manassas, VA). Constructs for expression of the following N-terminally tagged proteins were generated by subcloning into vector pCS2: HA- and CHY-dASUN; HA- and Myc-mASUN; and HA-, Myc-, and CHY-LIS1. The HA-LIS1 expression construct was a gift from Deanna Smith (University of South Carolina Biological Sciences, Columbia SC). The GFP-BICD2 expression construct was a gift from A. Akhmanova (Hoogenraad *et al.*, 2001). Mobyle@Pasteur, version 1.0.4, was used to determine the percentage identities and similarities between ASUN proteins from different species.

Anti-ASUN antibody production

Two rabbit polyclonal antibodies (M-hASUN Ab and C-hASUN Ab) were raised using synthetic peptides corresponding to the following amino acid residues of hASUN: IIKDSPDSPEPPNKKPLVEC (619–637) and CSVNNRAELYQHLKEENG (678–694), respectively. Exogenous cysteine residues were added for conjugation and affinity purification purposes. After exsanguination, enzyme-linked immunosorbent assay–positive antisera were antigen-affinity purified to a final concentration of ~1 mg/ml.

Immunoblotting and coimmunoprecipitation

Lysates were prepared using nondenaturing lysis buffer (50 mM Tris-Cl, pH 7.4, 300 mM NaCl, 5 mM EDTA, 1% Triton X-100). After SDS–PAGE, proteins were transferred to nitrocellulose for immunoblotting using standard techniques. Immunoblotting was performed using the following primary antibodies: c-Myc (9E10, 1:1000), HA (CAS 12, 1:1000), β-tubulin (clone E7, 1:1000; Developmental Studies Hybridoma Bank), mCherry (1:500; Clontech), CENP-F (clone 14C10 1D8, 1:500; Abcam), DIC (clone 74.1, 1:500; Abcam), DMN (clone 25, 1:250; BD Biosciences, San Diego, CA), M-hASUN (1:300), and C-hASUN (1:500). BICD2 antibody (1:2500) was a gift from A. Akhmanova (Hoogenraad *et al.*, 2001). HRP-conjugated secondary antibodies (1:5000) and chemiluminescence were used to detect primary antibodies. For coimmunoprecipitation experiments, anti–c-Myc agarose beads (40 µl; Sigma-Aldrich) were incubated with lysates of transfected HEK293 cells (500 µg) for 1 h at 4°C with shaking and washed 3× in lysis buffer. Samples were boiled in 6× sample buffer, resolved by SDS–PAGE, and analyzed by immunoblotting.

Sucrose density gradients

HeLa cells were transfected with either NT or hASUN siRNA. At 3 d posttransfection, lysates were prepared using nondenaturing lysis buffer (as described earlier). Lysates were layered on top of sucrose gradients (5 ml) with equal volumes of 30, 20, 10, and 5% sucrose in PBS (137 mM NaCl, 7 mM Na_2HPO_4, and 3 mM NaH_2PO_4, pH 7.2). Samples were centrifuged at 46,000 rpm for 16 h in a swinging-bucket rotor (SW55ti; Beckman Coulter, Brea, CA). After centrifugation, fractions (167 µl) were collected and analyzed by immunoblotting. Molecular weight standards were obtained from Bio-Rad (Hercules, CA).

ACKNOWLEDGMENTS

We thank Anna Akhmanova, Tom Hays, Julie Brill, and Deanna Smith for expression constructs and antibodies; Irina Kaverina and Ryoma Ohi for helpful discussions; and Matthew Broadus for critical reading of the manuscript. This work was supported by National Institutes of Health Grant GM-074044 (to L.A.L.) and Research Training Grant 2T32HD007043 (to J.N.J.).

REFERENCES

Akhmanova A, Hammer JA 3rd (2010). Linking molecular motors to membrane cargo. Curr Opin Cell Biol 22, 479–487.

Anderson MA, Jodoin JN, Lee E, Hales KG, Hays TS, Lee LA (2009). Asunder is a critical regulator of dynein-dynactin localization during *Drosophila* spermatogenesis. Mol Biol Cell 20, 2709–2721.

Basto R, Lau J, Vinogradova T, Gardiol A, Woods CG, Khodjakov A, Raff JW (2006). Flies without centrioles. Cell 125, 1375–1386.

Beaudouin J, Gerlich D, Daigle N, Eils R, Ellenberg J (2002). Nuclear envelope breakdown proceeds by microtubule-induced tearing of the lamina. Cell 108, 83–96.

Beswick RW, Ambrose HE, Wagner SD (2006). Nocodazole, a microtubule de-polymerising agent, induces apoptosis of chronic lymphocytic leukaemia cells associated with changes in Bcl-2 phosphorylation and expression. Leuk Res 30, 427–436.

Bettencourt-Dias M, Rodrigues-Martins A, Carpenter L, Riparbelli M, Lehmann L, Gatt MK, Carmo N, Balloux F, Callaini G, Glover DM (2005). SAK/PLK4 is required for centriole duplication and flagella development. Curr Biol 15, 2199–2207.

Bolhy S, Bouhlel I, Dultz E, Nayak T, Zuccolo M, Gatti X, Vallee R, Ellenberg J, Doye V (2011). A Nup133-dependent NPC-anchored network tethers centrosomes to the nuclear envelope in prophase. J Cell Biol 192, 855–871.

Bourdon V, Naef F, Rao PH, Reuter V, Mok SC, Bosl GJ, Koul S, Murty VV, Kucherlapati RS, Chaganti RS (2002). Genomic and expression analysis of the 12p11-p12 amplicon using EST arrays identifies two novel amplified and overexpressed genes. Cancer Res 62, 6218–6223.

Burgess SA, Knight PJ (2004). Is the dynein motor a winch? Curr Opin Struct Biol 14, 138–146.

Dujardin DL, Barnhart LE, Stehman SA, Gomes ER, Gundersen GG, Vallee RB (2003). A role for cytoplasmic dynein and LIS1 in directed cell movement. J Cell Biol 163, 1205–1211.

Fuller MT (1993). Spermatogenesis. In: The Development of *Drosophila melanogaster,* ed. M Bate and A Martinez-Arias, Cold Spring Harbor, NY: Cold Spring Harbor Laboratory Press, 71–147.

Godin JD, Humbert S (2011). Mitotic spindle: focus on the function of huntingtin. Int J Biochem Cell Biol 43, 852–856.

Greenspan RJ (2004). Fly Pushing: The Theory and Practice of *Drosophila* Genetics, Cold Spring Harbor, NY: Cold Spring Harbor Laboratory Press.

Gunsalus KC, Bonaccorsi S, Williams E, Verni F, Gatti M, Goldberg ML (1995). Mutations in twinstar, a *Drosophila* gene encoding a cofilin/ADF homologue, result in defects in centrosome migration and cytokinesis. J Cell Biol 131, 1243–1259.

Hebbar S, Mesngon MT, Guillotte AM, Desai B, Ayala R, Smith DS (2008). Lis1 and Ndel1 influence the timing of nuclear envelope breakdown in neural stem cells. J Cell Biol 182, 1063–1071.

Holzbaur EL, Vallee RB (1994). DYNEINS: molecular structure and cellular function. Annu Rev Cell Biol 10, 339–372.

Hoogenraad CC, Akhmanova A, Howell SA, Dortland BR, De Zeeuw CI, Willemsen R, Visser P, Grosveld F, Galjart N (2001). Mammalian Golgi-associated bicaudal-D2 functions in the dynein-dynactin pathway by interacting with these complexes. EMBO J 20, 4041–4054.

Jaspersen SL, Winey M (2004). The budding yeast spindle pole body: structure, duplication, and function. Annu Rev Cell Dev Biol 20, 1–28.

Kardon JR, Vale RD (2009). Regulators of the cytoplasmic dynein motor. Nat Rev Mol Cell Biol 10, 854–865.

Kemphues KJ, Raff EC, Raff RA, Kaufman TC (1980). Mutation in a testis-specific beta-tubulin in *Drosophila*: analysis of its effects on meiosis and map location of the gene. Cell 21, 445–451.

Lacroix B, Maddox AS (2012). Cytokinesis, ploidy and aneuploidy. J Pathol 226, 338–351.

Lee LA, Lee E, Anderson MA, Vardy L, Tahinci E, Ali SM, Kashevsky H, Benasutti M, Kirschner MW, Orr-Weaver TL (2005). *Drosophila* genome-scale screen for PAN GU kinase substrates identifies Mat89Bb as a cell cycle regulator. Dev Cell 8, 435–442.

Lim HH, Zhang T, Surana U (2009). Regulation of centrosome separation in yeast and vertebrates: common threads. Trends Cell Biol 19, 325–333.

Lippincott-Schwartz J (2002). Cell biology: ripping up the nuclear envelope. Nature 416, 31–32.

Malone CJ, Misner L, Le Bot N, Tsai MC, Campbell JM, Ahringer J, White JG (2003). The *C. elegans* hook protein, ZYG-12, mediates the essential attachment between the centrosome and nucleus. Cell 115, 825–836.

McGrail M, Hays TS (1997). The microtubule motor cytoplasmic dynein is required for spindle orientation during germline cell divisions and oocyte differentiation in *Drosophila*. Development 124, 2409–2419.

McKenney RJ, Vershinin M, Kunwar A, Vallee RB, Gross SP (2010). LIS1 and NudE induce a persistent dynein force-producing state. Cell 141, 304–314.

Mische S, He Y, Ma L, Li M, Serr M, Hays TS (2008). Dynein light intermediate chain: an essential subunit that contributes to spindle checkpoint inactivation. Mol Biol Cell 19, 4918–4929.

Rubin GM, Spradling AC (1982). Genetic transformation of *Drosophila* with transposable element vectors. Science 218, 348–353.

Salina D, Bodoor K, Eckley DM, Schroer TA, Rattner JB, Burke B (2002). Cytoplasmic dynein as a facilitator of nuclear envelope breakdown. Cell 108, 97–107.

Schroer TA (2004). Dynactin. Annu Rev Cell Dev Biol 20, 759–779.

Shu T, Ayala R, Nguyen MD, Xie Z, Gleeson JG, Tsai LH (2004). Ndel1 operates in a common pathway with LIS1 and cytoplasmic dynein to regulate cortical neuronal positioning. Neuron 44, 263–277.

Sitaram P, Anderson MA, Jodoin JN, Lee E, Lee LA (2012). Regulation of dynein localization and centrosome positioning by Lis-1 and asunder during *Drosophila* spermatogenesis. Development 139, 2945–2954.

Splinter D *et al*. (2010). Bicaudal D2, dynein, and kinesin-1 associate with nuclear pore complexes and regulate centrosome and nuclear positioning during mitotic entry. PLoS Biol 8, e1000350.

Stebbings L, Grimes BR, Bownes M (1998). A testis-specifically expressed gene is embedded within a cluster of maternally expressed genes at 89B in *Drosophila melanogaster*. Dev Genes Evol 208, 523–530.

Stevens NR, Raposo AA, Basto R, St Johnston D, Raff JW (2007). From stem cell to embryo without centrioles. Curr Biol 17, 1498–1503.

Stuchell-Brereton MD, Siglin A, Li J, Moore JK, Ahmed S, Williams JC, Cooper JA (2011). Functional interaction between dynein light chain and intermediate chain is required for mitotic spindle positioning. Mol Biol Cell 22, 2690–2701.

Tanaka T, Serneo FF, Higgins C, Gambello MJ, Wynshaw-Boris A, Gleeson JG (2004). Lis1 and doublecortin function with dynein to mediate coupling of the nucleus to the centrosome in neuronal migration. J Cell Biol 165, 709–721.

Tanenbaum ME, Akhmanova A, Medema RH (2010). Dynein at the nuclear envelope. EMBO Rep 11, 649.

Vassilev LT (2006). Cell cycle synchronization at the G2/M phase border by reversible inhibition of CDK1. Cell Cycle 5, 2555–2556.

Wong R, Hadjiyanni I, Wei HC, Polevoy G, McBride R, Sem KP, Brill JA (2005). PIP2 hydrolysis and calcium release are required for cytokinesis in *Drosophila* spermatocytes. Curr Biol 15, 1401–1406.

Zhang X, Lei K, Yuan X, Wu X, Zhuang Y, Xu T, Xu R, Han M (2009). SUN1/2 and Syne/Nesprin-1/2 complexes connect centrosome to the nucleus during neurogenesis and neuronal migration in mice. Neuron 64, 173–187.